

## Determination of the refractive index of liquids at cryogenic temperature

R. Faoro, M. Bassu, and T. P. Burg

Citation: *Appl. Phys. Lett.* **113**, 081903 (2018); doi: 10.1063/1.5043370

View online: <https://doi.org/10.1063/1.5043370>

View Table of Contents: <http://aip.scitation.org/toc/apl/113/8>

Published by the [American Institute of Physics](#)

---

---

**AIP** | Conference Proceedings

Get **30% off** all  
print proceedings!

Enter Promotion Code **PDF30** at checkout



## Determination of the refractive index of liquids at cryogenic temperature

R. Faoro, M. Bassu, and T. P. Burg<sup>a)</sup>

Max Planck Institute for Biophysical Chemistry, Biological Micro- and Nanotechnology, Göttingen 37073, Germany

(Received 8 June 2018; accepted 8 August 2018; published online 23 August 2018)

In this work, we present a method for measuring the refractive index of liquids at cryogenic temperature by shearing interferometry. The method is self-calibrated and easy to use over the range from cryogenic to room temperature. We validated the accuracy of our approach by comparing the measured refractive index of liquid propane with data reported in the literature. Moreover, we measured the refractive indices of three as yet uncharacterized fluorinated liquids that are of great interest as immersion fluids in the field of cryogenic light microscopy. © 2018 Author(s). All article content, except where otherwise noted, is licensed under a Creative Commons Attribution (CC BY) license (<http://creativecommons.org/licenses/by/4.0/>). <https://doi.org/10.1063/1.5043370>

The refractive index is a fundamental property which is crucial for the development and characterization of optical systems. At room temperature, many different methods of measuring the refractive index of materials in solid and liquid states exist. At cryogenic temperature, on the other hand, only a few materials have been characterized and the refractive index tabulated.<sup>1</sup> This lack of knowledge has limited the development of cryogenic optical applications such as cryo-immersion microscopy, for which knowing the refractive index of the immersion fluid is crucial to correct spherical and chromatic aberrations. In recent years, different approaches for cryoimmersion microscopy have been implemented,<sup>2–5</sup> but they all share the same limitation: the refractive index of the immersion fluid at the operating temperature is unknown and could be guessed only from the data available at RT. In our previous work,<sup>5</sup> we performed cryo-immersion microscopy at 133 K by using a water immersion objective, modified to work in cryo-conditions, in combination with the immersion fluid HFE 7200. The need to know whether the refractive index at 133 K of this liquid matches the refractive index of water at room temperature motivated us to find a simple way of measuring the refractive index of liquids in cryo-conditions.

Despite a large number of methods available for measuring the refractive index at room temperature, only a few approaches have been applied at cryogenic temperature.

In 1937, Grosse and Linn<sup>6,7</sup> adapted an Abbe refractometer to work down to 190 K. In this method, the refractive index was estimated by measuring the critical angle (*i.e.*, the total internal reflection angle) at the interface between the liquid under investigation and a prism of known refractive index. Using this system, they have been able to measure the temperature dependence of the refractive index of different fluids and liquefied gases. In the same year, Johns *et al.*<sup>8,9</sup> measured the refractive index of cryogenic liquids using an evacuated cell immersed in the liquid under investigation. This method, also based on the measurement of the critical angle, allowed measuring the refractive index down to liquid Helium temperature.

More recently, measurements of the angle of deviation of a monochromatic beam refracted by a cryogenic liquid

contained in a prism have been used. The refractive index of the cryogenic liquid contained in the prism was estimated using the angle of the prism and the measured angle of deviation of the beam. In the approach proposed by Smith,<sup>10,11</sup> the prism containing the liquid was rotated up to minimize the displacement of the refracted monochromatic beam with respect to the incident beam (principle of the minimum deviation). The apparatus was designed to measure refractive indices of inert gases over the temperature range of 77 to 273 K and at pressures up to 100 atm. Wong and Anderson<sup>12</sup> instead used a fixed truncated prism with a laser beam incident normally on the prism. The cryostat containing the truncated prism has been used for refractive-index measurements of liquids in the temperature range of 130–260 K.

Interferometric methods have also been applied for measuring the refractive index at cryogenic temperature. Diller used a Fabry-Perot resonator<sup>13</sup> to measure the refractive index of liquid and gaseous hydrogen. The resonator placed inside a cryostat was immersed in hydrogen. The state of hydrogen was changed by varying both temperature (15–298 K) and pressure (up to 230 atm). Zhang *et al.* used a Mach-Zehnder interferometer<sup>14</sup> where the liquid under investigation was contained in a cell placed on one of the two arms of the interferometer. The cell was cooled to 77 K using liquid nitrogen.

Interferometric methods usually reach higher precision than any diffraction or critical angle based methods. On the other hand, they are differential methods, and the refractive index must be referred to a known medium, usually air or vacuum.<sup>15</sup>

Most of the methods so far presented require complicated experimental setups where the optical parts are cooled at cryogenic temperature. Heating and cooling cycles between cryogenic and room temperature expose the optical parts to mechanical stress, which could lead to damage.

In this work, we report on the measurement of the refractive index of liquids at cryogenic temperature by using a shearing interferometric microscopy technique called Total Interference Contrast (TIC). In this technique, all the optical components are kept at room temperature, while the temperature of the liquid under observation varies between room and cryogenic temperatures. We used a commercially available system consisting of a TIC slider (ZEISS 1105-190) and

<sup>a)</sup>Electronic mail: [tburg@mpibpc.mpg.de](mailto:tburg@mpibpc.mpg.de)

a reflector module (ZEISS C DIC/TIC ARC P&C) installed on an upright microscope (ZEISS Axio Scope.A1) equipped with a compact mercury light source (HPX 120, LEJ). The wavelength of the light source was selected using a bandpass filter with a central wavelength of 590 nm and a FWHM of 10 nm (THORLABS FB590-10).

The TIC generates interference between two laterally sheared and orthogonally polarized images of the same object. This technique is similar to Differential Interference Contrast (DIC) microscopy used to enhance contrast while imaging biological samples or to detect thin layers ( $\sim 100$  nm) otherwise invisible in light microscopy. The main difference is that TIC uses a wider splitting angle than DIC, allowing a wider separation of the two images. Figure 1 shows a general schematic of the TIC working principle.<sup>16,17</sup> A Normaski prism splits the incident polarized light into two sheared orthogonally polarized beams which are focussed on the sample by the objective lens (ZEISS EC EPIPLAN 10 $\times$ /0.2 HD). The beams follow the reverse path, with a second passage through the prism, filtered by the analyzer, and reach the detector plane. The beams form two superimposed images of the sample surface, covered by the interference pattern generated by the difference in the optical path of the two beams induced by the prism. Under monochromatic illumination, the interference pattern shows a maximum every time the optical path difference is a multiple of  $\lambda$ .

Figure 1(b) shows an example of the interference pattern generated by imaging a sample consisting of a gold coated silicon chip with a groove ( $1.5 \pm 0.1 \mu\text{m}$  in depth,  $70 \pm 0.1 \mu\text{m}$  in width) in the middle [see Fig. 1(c)]. The inter-fringe distance, labeled with  $a$ , is related to the path difference and remains invariant over the image. The interference pattern is shifted at the two steps by a distance, labeled with  $b$ , due to

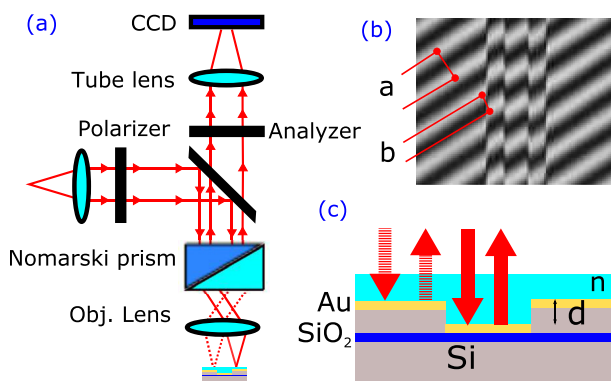


FIG. 1. (a) The refractive index is measured using a shearing interferometry technique known as Total Interference Contrast (TIC) microscopy that allows measuring the difference in the height and/or refractive index of the specimen. This method measures the optical path difference between two laterally shifted, orthogonally polarized images of the same object. As shown in the left part of the image, the illumination source is circularly polarized, and the split of the incident polarized light by a Normaski prism into two sheared orthogonal polarized beams that are focused on the sample under investigation is also shown. The two reflected beams are then recombined by the Normaski prism and filtered by a second polarizer called an analyzer. (b) Example of the interference pattern generated by imaging a sample consisting of a gold coated silicon chip with a groove in the middle. The inter-fringe distance is labeled with  $a$ , while  $b$  is the shift induced by the groove step. (c) Schematic of the golden coated silicon chip. The groove is  $1.5 \pm 0.1 \mu\text{m}$  in depth and  $70 \pm 0.1 \mu\text{m}$  in width. The dashed and full arrows show the difference in the optical path of the two orthogonal polarized beam.

the optical path difference  $\Delta = 2n \times d$ , where  $d$  is the groove depth and  $n$  is the refractive index of the medium. The optical path difference  $\Delta$  can also be expressed as a function of wavelength  $\lambda$ , inter-fringe distance  $a$ , and shift  $b$ , yielding<sup>18,19</sup>

$$n \times d = \left(m + \frac{b}{a}\right) \frac{\lambda}{2}, \quad (1)$$

where  $m$  is an integer number. As the shift  $b$  has a periodicity of  $\lambda/2$ , the integer  $m$  can be determined by knowing  $n \times d$  with a precision within  $\lambda/4$ .

In order to measure the refractive index of liquids at temperatures ranging between room temperature and cryogenic temperature, the structured gold coated silicon chip was mounted inside a recess within a massive aluminum holder (see Fig. 2). A small chamber closed with a thin microscope slide and an O-ring contained the liquid under investigation. The aluminum holder was cooled by immersing it into liquid nitrogen. A sensor PT-100 glued in close proximity of the silicon chip was used to monitor the temperature. Intermediate temperatures are reached letting the holder warm up through thermal exchange with the surrounding environment. The instantaneous temperature uniformity of the liquid in the chamber was assured by the relatively large mass of the aluminum holder. This is crucial for the reliability of the measurement, as a temperature gradient would affect the interference pattern and thus the final results of the refractive index measurement.<sup>20</sup>

The refractive index of liquefied gases and cryogenic liquids that are also liquid at room-temperature could be measured. All liquids to be measured were first pre-cooled in a vial embedded in the aluminum holder. Image acquisition and temperature measurement were synchronized using Labview.

Every session of the measurement starts with the determination of the depth  $d$  with sub-nanometric precision by measuring at room temperature the optical path  $n \times d$  while flowing nitrogen gas ( $n = 1.0003$ ) into the system.

The method was validated by measuring the refractive index of propane at temperatures below the boiling point of

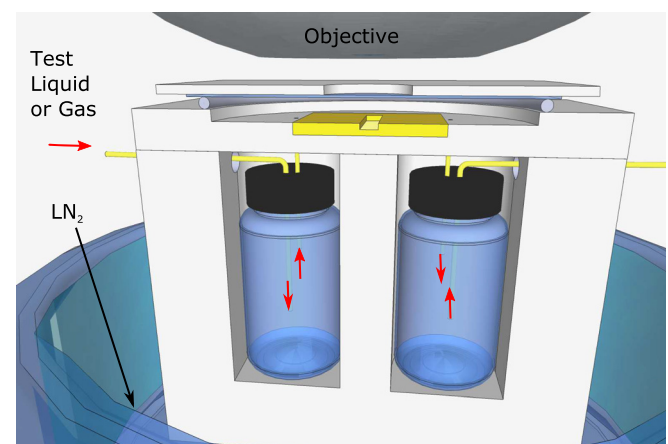


FIG. 2. Scheme of the TIC sample cryostage: the manifold is cooled by immersion in liquid nitrogen and equipped with two fluid reservoirs that act as a liquefaction chamber (RT gas) or a precooling chamber (RT liquid). The substance under investigation is pressure driven to the upper chamber, where our golden coated trench is placed. The temperature of the system is measured by a PT-100 placed close to the sample.

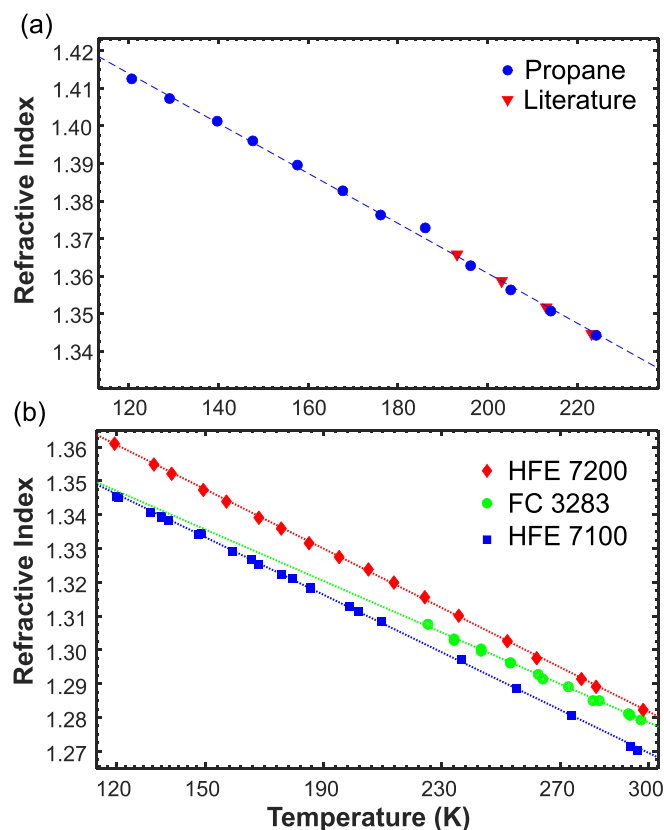


FIG. 3. (a) Refractive index of liquid propane at different temperatures measured by the TIC technique. The data extrapolated agree with the value reported by Grosse and Linn<sup>7</sup> within 0.005 RI unit, validating the measurement system. The data show a linear dependence on the temperature. (b) Refractive index of the fluorinated immersion liquids. Any liquid shows a linear dependence with the temperature as expected, indicating the absence of the phase change in the temperature range investigated.

231 K. The refractive index shows a linear inverse dependence on the temperature, with a slope of  $-6.4 \pm 0.2 \times 10^{-4}$  RIU/K, which is in good agreement with the data available in the literature for liquefied propane [red triangles in Fig. 3(a)],<sup>7</sup> demonstrating the accuracy of the method.

Furthermore, we measured the refractive index of three liquids of which the refractive index is known only at room temperature: the partially fluorinated methoxy-nonafluorobutane (3M<sup>TM</sup> HFE 7100) and ethoxy-nonafluorobutane (3M<sup>TM</sup> HFE 7200) and the fully fluorinated perfluorotripropylamine (3M<sup>TM</sup> FC 3283).

HFE 7200 and HFE 7100 have a pour point of 135 K and 138 K, respectively. We were able to measure the refractive index of the two liquids at temperatures down to 119 K because even below the pour point, they are transparent. The measured refractive indices at room temperature ( $n = 1.282 \pm 0.003$  at 298 K for HFE 7200 and  $n = 1.269 \pm 0.003$  at 296 K for HFE 7100) are in good agreement with the values calculated by Ando using the density functional theory ( $T = 298$  K,  $\lambda = 590$  nm, HFE 7200  $n = 1.282$ , and HFE 7100  $n = 1.265$ ).<sup>21</sup> The refractive indices of both the liquids show an inverse dependence on temperature with a slope of  $-4.38 \pm 0.03 \times 10^{-4}$  RIU/K for HFE 7200 [red rhombi in Fig. 3(b)] and

$-4.25 \pm 0.03 \times 10^{-4}$  RIU/K for HFE 7100 [blue squares in Fig. 3(b)]. The similarity between the two slopes is not surprising since the two liquids are chemically very similar. It is worth noticing that, for both HFE 7200 and HFE 7100, there are no changes in the linear behavior for temperatures below the liquid pour point, which would be expected in the presence of a phase change.<sup>22</sup>

The refractive index of FC 3283 was measured in the range between room temperature and 223 K, which is the pour point of the liquid. Below this temperature, the liquid is not transparent, and it is not possible to measure the refractive index. The data plotted in Fig. 3(b) (green circles) show a linear inverse dependence of the refractive index on temperature with a slope of  $-3.8 \pm 0.1 \times 10^{-4}$  RIU/K. The refractive index  $n = 1.279 \pm 0.003$  measured at 297 K is in agreement with the data reported in the literature.<sup>23</sup>

Our results show that TIC microscopy can be exploited for measuring the refractive index of liquids and liquified gases at cryogenic temperature with a precision down to  $3 \times 10^{-3}$  RIU. Moreover, the results obtained by measuring the refractive index of HFE 7200, which we used in a previous work as immersion fluid for cryo-immersion microscopy at 133 K,<sup>5</sup> provide us important insights into the behavior of the optical system and will allow an improvement of the system. Future work will be devoted to improving the precision of the method and to measuring the refractive index of more liquids at different wavelengths.

<sup>1</sup>B. W. C. Wohlfarth, in *Refractive Indices of Organic Liquids, Landolt-Börnstein-Group III Condensed Matter*, edited by M. D. Lechner (Springer-Verlag, Berlin/Heidelberg, 1996), Vol. 38B.

<sup>2</sup>M. A. Le Gros, G. McDermott, M. Uchida, C. G. Knoechel, and C. A. Larabell, *J. Microsc.* **235**, 1 (2009).

<sup>3</sup>M. Metzger, A. Konrad, S. Skandary, I. Ashraf, A. J. Meixner, and M. Brecht, *Opt. Express* **24**, 13023 (2016).

<sup>4</sup>M. Nahmani, C. Lanahan, D. DeRosier, and G. G. Turrigiano, *Proc. Natl. Acad. Sci.* **114**, 3832 (2017).

<sup>5</sup>R. Faoro, M. Bassu, Y. X. Mejia, T. Stephan, N. Dudani, C. Boeker, S. Jakobs, and T. P. Burg, *Proc. Natl. Acad. Sci.* **115**, 1204 (2018).

<sup>6</sup>A. V. Grosse, *J. Am. Chem. Soc.* **59**, 2739 (1937).

<sup>7</sup>A. V. Grosse and C. B. Linn, *J. Am. Chem. Soc.* **61**, 751 (1939).

<sup>8</sup>H. E. Johns and J. O. Wilhelm, *Can. J. Res.* **15a**, 101 (1937).

<sup>9</sup>E. F. Burton, *Nature* **140**, 1015 (1937).

<sup>10</sup>C. P. Abbiss, C. M. Knobler, R. K. Teague, and C. J. Pings, *J. Chem. Phys.* **42**, 4145 (1965).

<sup>11</sup>B. L. Smith, *Rev. Sci. Instrum.* **34**, 19 (1963).

<sup>12</sup>L. Y. Wong and A. Anderson, *J. Opt. Soc. Am.* **62**, 219 (1972).

<sup>13</sup>D. E. Diller, *J. Chem. Phys.* **49**, 3096 (1968).

<sup>14</sup>J. H. Zhang, S. R. Bao, R. P. Zhang, and L. M. Qiu, *IOP Conf. Ser.: Mater. Sci. Eng.* **101**, 012190 (2015).

<sup>15</sup>J. D. Olson and F. H. Horne, *J. Chem. Phys.* **58**, 2321 (1973).

<sup>16</sup>D. L. Lessor, J. S. Hartman, and R. L. Gordon, *J. Opt. Soc. Am.* **69**, 357 (1979).

<sup>17</sup>C. J. Cogswell and C. J. R. Sheppard, *J. Microsc.* **165**, 81 (1992).

<sup>18</sup>C. Kuncser, A. Kuncser, and S. Antohe, *Rom. Rep. Phys.* **64**, 143 (2012).

<sup>19</sup>M. Vaupel, A. Dutschke, U. Wurstbauer, F. Hitzel, and A. Pasupathy, *J. Appl. Phys.* **114**, 183107 (2013).

<sup>20</sup>O. Bryngdahl, *J. Opt. Soc. Am.* **53**, 571 (1963).

<sup>21</sup>S. Ando, *J. Photopolym. Sci. Technol.* **19**, 351 (2006).

<sup>22</sup>S. G. Warren, *Appl. Opt.* **23**, 1206 (1984).

<sup>23</sup>*Handbook of Data on Common Organic Compounds, III*, edited by D. R. Lide and G. W. A. Milne (CRC Press, Inc., Boca Raton, FL, USA, 1994), Vol. 5, p. 4266.